Thermal plasticity of the circadian clock is under nuclear and cytoplasmic control in wild barley

Eyal Bdolach[1,2], Manas Ranjan Prusty[1], Adi Faigenboim-Doron[1], Tanya Filichkin[3], Laura Helgerson[3], Karl J Schmid[4], Stephan Greiner[5], Eyal Fridman[1]

[1]Plant Sciences Institute, Volcani Agricultural Research Organization (ARO), Bet Dagan, Israel

[2] Department of Life Sciences, Ben-Gurion University, 84105, Beer-Sheva, Israel

[3] Crop & Soil Science Dept., Oregon State University, Corvallis, OR U.S.A.

[4] Institute of Plant Breeding, Seed Science and Population Genetics, University of Hohenheim, Stuttgart, Germany

[5] Max-Planck-InstitutfürMolekularePflanzenphysiologie, Am Mühlenberg 1, D-14476 Potsdam-Golm, Germany

Author for correspondence:

Eyal Fridman

Institute of Plant Sciences, Agricultural Research Organization (ARO), The Volcani Center, P. O. Box 6, 5025001, Bet Dagan, IsraelE-mail: fridmane@agri.gov.il, Tel: +972-3-9683901

Highlight

Circadian clock robustness to high temperature is controlled by nuclear and plasmotype quantitative trait loci in wild barley (*Hordeum vulgare* ssp. *spontaneum*) reciprocal doubled haploid population

Abstract

Temperature compensation, the ability to maintain the clock characteristics (mainly period) in face of temperature changes, is a considered a key feature of circadian clock systems. In this study, we explore the genetic basis for the circadian clock plasticity under high temperature by utilizing a new doubled haploid (DH) population derived from two reciprocal *Hordeum vulgare* sps. *spontaneum* hybrids genotypes (B1K-50-04 and B1K-09-07). Genotyping by sequencing of DH lines indicate a rich recombination landscape with minor fixation (less than 8%) for one of the parental allele, yet with prevalent and varied segregation distortion across seven barley chromosomes. Phenotyping this population was conducted with a high-throughput platform under optimal and high temperature environments. Genetic analysis by different ways, including QxE and binary-threshold models, identified significant influence of the maternal organelle genome (the plasmotype), as well as few nuclear quantitative trait loci (QTL), on clock phenotypes (free-running period and amplitude). Moreover, it showed a differential contribution of cytoplasmic genomes to buffering of the clock rhythm against high temperature. Resequencing of the parental chloroplast indicate the presence of few candidate genes underlying these significant effects. This first reported plasmotype-driven clock plasticity paves the way for identifying hitherto unknown role of nuclear and plasmotype variations on clock robustness and on plant adaptation to changing environments.

Key words: Adaptation, Plasticity, Canalization, Circadian clock, QTL by Environment Interactions, Plasmotype, Wild barley

Introduction

Radiation and adaptation of plant populations has consequences to the genetic make-up of both nuclear and organelle genomes, owing to selective forces as well as stochastic genetic drift and founder effects. One of the great challenges in evolutionary biology is to distinguish between neutral and causal genetic variation that participate in this interplay between genetic and phenotypic variation, while gaining better understanding of the mechanism underlying the observed plasticity. Identification of the genetic network regulating phenotypic plasticity is a key for deciphering these mechanisms, as well as for following the trajectory of their alleles across range of habitats and understanding the adaptation history of a species (Price et al., 2003).

Circadian clock rhythm, which controls the pace and diurnal timing of plant development, physiology and biochemistry is considered a key adaptive trait for the sessile plants (Dodd et al., 2005)(Greenham and McClung, 2015). Nevertheless, there are few studies that have utilized naturally occurringcircadian clock variation in large populations to realize if robustness or flexibility is more beneficial against increased temperatures. This is perhaps due to the fact that most of our understanding of the genes and network involved in regulation of the circadian rhythms are based on mutant phenotypes. Nevertheless, in Arabidopsis a genomic dissection in recombinant inbred lines (RILs) of Columbia by Landsberg *erecta* (CoL) and Cape Verde Islands by Landsberg *erecta* (CvL) identified contribution of clock and non-clock genes to variation in circadian clock rhythms (Edwards et al., 2005). In addition, analysis in Arabidopsis accessions of the responses to elevated temperature under controlled experimental conditions indicates the presence of naturally occurring variation in their buffering capacity against high temperature in this model species (Kusakina et al., 2014). This might represent adaptation to different temperature regimes in their original niche. Temperature compensation, the ability to maintain the clock characteristics (period and amplitude) in face of temperature changes, is considered a key feature of circadian clock systems (Johnson et al., 2003). However, Arabidopsis plants do speed their clock in response to high temperatures (Edwards et al., 2005) (Kusakina et al., 2014), although the picture emerging from analysis of clock genes as biomarkers for the clock plasticity indicate varying responses with regard to changes in their absolute values and in their dynamics. For example, although *CCA1* and *LHY*

transcription shorten considerably across all Arabidopsis accessions in transition from 17°C to 27°C, the temperature effects on *LHY* period were shown to be accession specific (Kusakina et al., 2014).

Mostly based on molecular mutant phenotypes it was demonstrated that CCA and LHY function in buffering the clock under low or high temperature, respectively (Gould et al., 2006). Yet, attempts to find an association between genetic variation of these two genes, as well as in 7 more clock genes, and temperature-dependent modulation of growth (as proxy for fitness) did not find any match (Kusakina et al., 2014). These results indicate that there are other genes outside the core clock machinery governing this relationship between reduced buffering of the clock (Edwards et al., 2005), and that the correlation could be found in other fitness-traits as suggested by Kusakina et al. (Kusakina et al., 2014). One source for such causal genetic variation is the natural divergence of the cytoplasmic genomes (plastid and mitochondria), a source currently completely overlooked.

Recent work could demonstrate that variation in the organellar genome can contribute to phenotypic or metabolomic differences between individuals, although the relative contribution of organellar genes versus nuclear genes remains unclear (Joseph et al., 2013). Moreover, effects of the cytoplasm on plant fitness and agronomic traits is known since beginning of the 20th century, after discovered by the German botanist Carl Correns (1909)(Roux et al., 2016)(Greiner and Bock, 2013). Probably the most prominent example is cytoplasmic male sterility (CMS), which is heavily used for hybrid seed production (Luo et al., 2013). Disease resistance could also be influenced by the genotype of the cytoplasm, the plasmotype. Moreover, especially in grasses the contribution of the plasmotype to yield and grain quality has been demonstrated (Frei et al., 2003)(Sanetomo and Gebhardt, 2015). Likely these traits are a result of a local adaption of the original wild alleles, since for example in bread wheat (*Trictium aestivum*) cytoplasmic influence on fruit quality is influenced by genotype-by-environment interactions (Ekiz et al., 1998)(Frei et al., 2003). Vis-à-vis regulation of the circadian clock rhythm it was shown that mutations in nuclear-encoded chloroplast proteins (GUN1) known to be involved in retrograde signaling, or in mRNA maturation in chloroplast, are feeding back into the nucleus and affect the expression of both oscillator (e.g. CCA1) and output genes (CAB) of the circadian clock (Hassidim et al., 2007). Similarly, photosynthetic electron transport generates a retrograde signal that adjusts the alternative splicing of nuclear-encoded transcripts

encoding an SR protein (a regulator of RNA splicing) and other splicing factors (Petrillo et al., 2014). The nature of the signal and whether it is circadian-regulated is unknown, but an interesting hypothesis is that circadian regulation of photosynthesis within chloroplasts may cause circadian modulation of a retrograde signal that alters nuclear mRNA splicing (Dodd et al., 2015).

The wild barley (*Hordeum vulgare* sps. *spontaneum*) is an attractive and emerging model species in plant evolutionary biology, especially to address questions related to adaptation and evolutionary biology processes (Hubner et al., 2009). This is mainly due to its wide and well-defined geographic distribution(Pankin et al., 2018)(Russell et al., 2016), as well as the availability of full genome sequence and resequencing pipelines (Mascher et al., 2013)(Wendler et al., 2014)(Mascher et al., 2017). In addition, a huge genetic toolbox including the possibility of generating doubled haploids for genetic dissection, is available (Touraev et al., 2009). The core distribution range of wild barley is the Fertile Crescent, but it extends from western North Africa to the eastern Himalayas (Harlan and Zohary, 1966)(Badr et al., 2000)(Russell et al., 2016) thus spanning a broad ecological range. The Barley1K (B1K) collection was sampled during spring of 2007 along the distribution range of wild barley in Israel in a hierarchical sampling mode (https://sites.google.com/site/barley1k/; (Hubner et al., 2009). Comparisons of the phenotypic variation between cultivated and wild barley, and within wild barley gene pool, identified three main phenotypic clusters, namely the Coastal, Northern and Desert ecotypes (Hübner et al., 2013). A more recent study, conducted with a subset of B1K genotypes, found that circadian clock traits are also correlated with the climatic variation at the Barley1K sites (Dakhiya et al., 2017).

As part of our attempt to understand the causal variation for the genetic and phenotypic differences found in the B1K population (Hübner et al., 2012) (Hübner et al., 2013)(Bedada et al., 2014), including the significance of organelle genome variation, we have generated a doubled haploid population. The 121 homozygous lines areoriginated from two reciprocal F1 hybrids betweentwo B1K accessions with distinct phenology and phenotypic plasticity. Here, we partitioned the diversity and plasticity of the circadian clock rhythm among the DH population. To that end, we have scaled-up the recently developed prompt chlorophyll fluorescence (F) methodology for determining circadian rhythms (Dakhiya et al., 2017) to ultra-throughput phenomics tools (SensyPAM). This platform allowed examining all

population under two temperature (optimal and high) for free running period (FRP) and amplitude (AMP) of circadian clock under continuous light. Furthermore, it allowed us to examine the contribution of variation at nuclear loci, organelle variation and their interaction to clock traits variation, as well on genetic control of robustness of these rhythms against high temperature.

Materials and Methods

Plant material

One hundred and twenty one doubled haploids (DH) were derived from the F1 generation of the cross between B1K-50-04 and B1K-09-07, both accessions are single seed descent from the original Barley1K collection (Hubner et al., 2009). Spikes taken from two derived F2 plants were used to generate DH following the anther culture protocol described by Cistué et al. (Cistué et al., 2003). Eighty-one DH were derived from an F1 in which the female donor was B1K-50-04 and the other forty from the reciprocal hybrid (Table S1). The 121 doubled haploids, referred to as the Ashkelon-Hermon (ASHER) population, are available to the research community upon request.

Read mapping, SNP discovery, genotype calling and filtering for nuclear loci

Raw fastq files were processed with the standalone TASSEL 5 GBS v2 pipeline (Glaubitz et al., 2014) preparation for alignment and SNP discovery. Prior to the alignment steps, the reads were trimmed to 64 bases. Reads were then collapsed into a set of unique sequence tags. Short reads were mapped on the *Hordeum vulgare* genome assembly reference v2, available in the Gramene database (ftp://ftp.gramene.org/pub/gramene/release-56/fasta/hordeum_vulgare/dna/) using BWA 0.7.12-r1039 (Li and Durbin, 2009) with default parameters. SNP discovery and production were performed with the standalone TASSEL-GBS. Only uniquely aligned reads were considered for SNP calling. Genotype calling was carried out with the TASSEL-GBS plugins 'DiscoverySNPCallerPluginV2' and 'ProductionSNPCallerPluginV2' with minimum minor allele frequency of 0.01. Perl scripts were used to filter the 60,845SNP markers resulting from TASSEL-GBS pipeline (Table S2). Due to the homozygous nature of a DH population we discarded all markers with heterozygotes parents from the analysis and only allowed different

genotype between the parents. We also excluded markers exhibiting three and four alleles in the whole dataset (resulted with 2,327 SNPs; Table S3; Fig. 1).

For QTL mapping we applied fourfiltering criteria to select core set of markers: 1) heterozygous SNPs were omitted since this is not expected for a DH population, 2) there were at least 90 DH scored for the SNP, 3) there was minimal allele frequency of 10% among DH, 4) adjunct SNPs with identical pattern across DH were represented with one of them. This procedure led to a list of 760 high-confidence nuclear SNPs used to characterize the genetic make-up and allow QTL mapping (Table S3). Furthermore, prior to the QTL mapping a linkage map was calculated for these 760 markers to position them on the 7 barley chromosomes (Fig. S1). In addition, to determine possible allelic distortion, a Chi-square test was performed against the null hypothesis of a 1:1 ratio between the A and B alleles in each locus.

Plastid genome (plastomes) sequencing and SNP discovery

Illumina paired-end libraries (375 bp insert size) of total barley DNA were used to sequence the plastid genomes of the parental lines B1K-50-04 and B1K-09-07. For this, 250-bp reads were mapped against the barley reference plastomes of the cultivar Barke (KC912687; (Middleton et al., 2014)) by employing the SeqMan NGen v.14.1.0 (DNASTAR, Madison, WI, USA) software. Larger insertions/deletions were identified by paired-end mapping. The finished plastid DNA contigs (comprising of LSC, IR_B and SSC, with an average coverage of 234 and 331, respectively) were annotated with GeSeq v.1.20 (Tillich et al., 2017) and SNPs called in SeqMan Pro v15.0.1 (DNASTAR, Madison,WI, USA).

Circadian clock phenotype of doubled haploids under optimal and high temperature

To mimic the natural conditions of the wild barley population grown in the Southern Levant, where the original Barley1K infrastructure was collected (Hubner et al., 2009), we have amend the previous protocol for measuring free running clock measurements under continuous light by fluorescence (F) measurements (Dakhiya et al., 2017). Mainly, instead of growing the seedling under regime of 16 h light and 8 h dark, plants were grown to the emergence of the fourth leaf under 8h light and 16h dark under a constant temperature of 20°C. Following this entrainment of the plants they were moved to a high-throughput SensyPAM (SensyTIV, Aviel, Israel) that was

custom designed to allow F measurements for up to 240 plants every experiment. The SensyPAM includes a large carousel suitable for 14 plastic trays (Fig. S2A) that spinning to the imagingchamber (Fig. S2C). Each tray is filled with water and can contain up to 24 plants that are put along the sides of the tray and the fully expanded upper leaves is pinned down to a black sponge. The imaging chamber is installed with acA-1920-40um CCD camera (Basler, Exton, PA, US) with 647nm long pass edge filter (Semrock, Rochester, New York, US) and LED light panel. The LEDs are royal blue (450 nm), red-orange (630 nm), far-red (740 nm) and cool white (450-700 nm) (REBEL type, Lumiled, San Jose, CA, US). Before the tray is photographed it is kept at a dark adaptation chamber for two steps (10 min.) (Fig. S2B), thereafter it is moved for three more min. at the imaging chamber (Fig. S2C; total 13 min. dark adaptation) followed by the timeline of light pulses. To identify the individual plants 3-4 areas of interest (AOI) are marked in the SensyPAM software for each leaf before the experiment begins (Fig. S2D). The light pulses and durations are similar to that of the saturation pulse method (Schreiber, 2004) with saturating flashes of 1600 µmoll m^2 s^{-1} and actinic light of 457 µmoll m^2 s^{-1} (example output in Fig. S2E). The F parameters, and light durations are explained in Table S5. The SensyPAM is located in a room with controlled temperature and light. In the ASHER DH population different plants were grown under optimal temperature (OT, 22°C) and high temperature (HT, 32°C) in several cycles of experiments (Fig. S3). For the clock measurement F is measured every 2.5 hours for 3 days in light. Each genotype was grown twice in each temperature with 4 plants included in each round. For the clock analysis we calculated mean NPQlss ((Fm-Fmlss)/Fmlss) and extracted the period, amplitude and relative amplitude error (RAE)in the BioDare2 website (https://biodare2.ed.ac.uk) (Fig. S2F). Input Data "cubic dtr" and Analysis Method "MFourFit" (Zielinski et al., 2014). To understand therobustness of these rhythms against high temperature we calculated the delta of the free-running-period (FRP) and amplitude (AMP) between the two temperatures (HT-OT). In a different approach we analyzed the variance of the FRP means between the two treatments with t Student's test, per DH line and converted the difference between the temperatures to a categorical binary vector (environmental response FRP; erFRP). If the difference was significant ($p<0.01$) the response is 1 and 0 if not. This approach takes into account the variance in each line per temperature.

Genome-wide and cytonuclear interaction QTL analysis

The genome wide and di-genic (nuclear and cytonuclear) QTL interaction analysis of the DH population for different traits was carried out using inclusive composite interval mapping (ICIM; (Li et al., 2007)) with software package IciMapping V4.1(Meng et al., 2015). The IciM 4.1 uses an improved algorithm of composite interval mapping for biparental pupation. It has a high detection power, reduced false detection rate and less biased estimates of the QTL effects which minimizes the bias for small population size. Initially a BIN function was used to remove the redundant markers. Linkage map was constructed using the MAP function of the software with the steps (parameters) as grouping (by anchor order), ordering (by input), and rippling (with SARF, window size = 5) and using Kosambi mapping function (Fig. S1). The output from the MAP was used for finding the QTLs for the different traits with BIP function. For the additive analysis, and digenic epistasis interaction, mapping step of 1.0 cM with a probability in stepwise regression (PIN) value of 0.001 was used with the parameters: missing phenotype = deletion, step = 1 cM, and probability in stepwise regression = 0.001. To identify significant QTL, LOD score of 2.5 was set manually at a significance level of $P < 0.05$ as well as the threshold LOD was obtained by performing a 1000-permutation test. The digenic epistatis interactions were estimated at both LOD value of (2.5) and (5). The QTL by environment interaction (QxE) was also performed with the inclusive composite interval mapping (ICIM) method using the MET function of the software QTL IciMapping 4.1 (Li et al., 2007, Meng et al., 2015). To study the cytonuclear interaction, the cytoplasm genome was considered as an extra chromosome (plasmotype) in addition to the 7 nuclear chromosomes of barley and was used for the QTL and epitasis analysis.

Results

The nuclear and plastid genome variation within the Ashkelon-Hermon (ASHER) wild barley doubled haploid population

To explore potential link between genetic diversity and circadian clock robustness to changing environments 121 homozygous doubled haploid (DH) were generated from a reciprocal cross between B1K-09-07 and B1K-50-04. The two accessions are originated from two different habitats of wild barley in the Southern Levant, a most allelic rich part of the *H. spontaneum* gene pool (Pankin et al., 2018). The DH procedure was making use of anthers taken from two F2 plants derived of two reciprocal F1 hybrids between the parental lines (see Methods). This yielded a total of 81 and 40 DH lines with B1K-50-04 or B1K-09-07 cytoplasm, respectively (Table S1).

Illumina genotype by sequencing of the 121 lines compared to the DNA of the parental lines yielded c. 52 million reads, out of which on average 81.8 % matched the *Hordeum vulgare* genome assembly reference v2 (ftp://ftp.gramene.org/pub/gramene/release-56/fasta/hordeum_vulgare/dna/)(Table S2).The ASHER doubled haploid population descended from two single reciprocal F_2 genotypes (see Methods), and this could be seem clearly in their phylogeny in which the DH descended from each origin clustered together (Fig. 1). To examine the possibility that selection (in F1 or F2 generations), or genetic drift (in F2 generation), could occur during the process of selecting two F2 individuals and culturing male gametes and anthers to produce double haploid plantlets(Cloutier et al., 1995), the genome-wide allele frequency was analyzed. It is expected that differential selection will manifest itself in segregation distortion that is departure from the expected 1:1 ratio of allele pairs in the progeny of the original F_1 individual at heterozygous loci (Nixon, 2006). Figure 2A and Table S3 depicts the segregation ratios across seven barley chromosomes among the 121 DH lines for a total of 2,237 markers that were different between two parental lines. In total there were 7.6% or 7.4% of the markers that drifted to allele frequency higher than 0.9 for the B1K-50-04 or B1K-09-07 allele, respectively (hereafter coded as ‘A’ or ‘B’ alleles for any locus). This pattern implies that the genomic landscape could cover a significant portion of the genome (app. 85%) for identifying causal variation for phenotype of interest. Nevertheless, transmission ratio distortion (TRD), or significant bias from the expected 1:1 ratio

between the two parental alleles in the DH progeny, was prevalent to both directions. The rate of significant TRD (Chi-test, P<8*10E-5, corrected to multiple testing) ranged from 10% of markers in chromosome 7 to 90% for chromosome 4 (Fig. 2B; Table S3).

Plastome variation between the parental lines of the reciprocal doubled haploid population

The SNP calling pipeline identified 81 SNPs between the plastid genomes of B1K-50-04 and B1K-09-07, including 40 singletons and 42 SNP indels ranging in size between one and eight nucleotides (Table S4). Notably, the number of polymorphism in coding regions between the parental lines (six non-synonymous and seven synonymous variants) exceeds the variation identified in earlier studies (Middleton et al., 2014). However, more careful analyses of sequence variation in the barley plastome should include a harmonization of gene annotations.

Carriers of the B1K-50-04 plasmotype show increased robustness of the circadian rhythm

To explore potential link between identity of the cytoplasm (chloroplast and mitochondria) and circadian rhythm, 114 of the ASHER-DH population were examined in a high-throughput manner for circadian clock rhythm by scaling-up the chlorophyll F method (Dakhiya et al., 2017) (see Methods; Fig. S2). In this analysis we asked whether plastid or mitochondria organelles (together referred to as plasmotype) could be involved in regulating the pace of the clock, as well as robustness of its characteristics. Initially, the plants were entertained under short days (8/16 L/D), which correspond to the natural winter day length of the B1K (see Methods). Plants F reflectance were extracted to calculate the non-photochemical quenching (NPQlss) during three days under continuous light and at two temperature regimes: 22°C (optimal temperature; OT) and 32°C (higher temperature; HT). NPQlss served to calculate the free-running-period (FRP) and amplitude (AMP) of the plants circadian clock (Dakhiya et al., 2017). These clock characteristics were compared between the two sub-populations, i.e. 0950 or 5009 DHs, derived from B1K-09-07 or B1K-50-04 as female parent in the original F1 hybrid, respectively, to address these questions.

Overall, clock rhythms ranged with FRP values between 21.5 to 31.7 h under OT, and a significantly narrower range under HT between 21.0 to 25.9 h (Fig. 3A). Next, we made three comparisons, i.e. between the temperature regimes and within the two sub-populations. The means FRP of the DH population differ significantly (Student's t-Test; $P<0.0001$) between the two temperatures, i.e. clock rhythm accelerated from 25.3 ±2.3 h under OT to 23.2±1.02h under HT (Fig. 3B I). The difference between the two sub-population FRP was highly significant under OT ($P<0.0001$), but not under HT ($P=0.11$; Fig. 3B II). The mean FRP of the sub-population 0950 was 26.5 ±2.2 h in OT and circadian clock significantly accelerated (shortened FRP) to 23.03 ±1.0 h under HT (Fig. 3B III). This is compared to mean FRP of the sub-population 5009 that was 24.7 ±2.05 h in OT and slightly accelerated to 23.35 ±1.0 h under HT (Fig. 3B III). In summary, there was a difference of more than 2 h (2.2 h) in the delta of the clock FRP (dFRP) between the carriers of the two cytoplasms. For further genetic mapping of clock plasticity (see below) we calculated the dFRP, i.e. the difference between mean FRP value under HT and OT, for each DH line. Comparison of these dFRP values between the carriers of the two sub-populations showed indeed a significant difference (Student's t-Test; $P<0.0001$). Altogether, these results implicate that the maternal genome of 5009 DHs confer circadian clock more robust or less plastic to HT.

Similar comparisons made for the clock amplitude (AMP), which showed a general and significant ($P<0.001$) doubling of the AMP level between high and lower temperature (0.032 in OT and 0.058 in HT; Fig. 3C I). However, under both temperatures there was not a significant AMP difference between two sub-populations (Fig. 3C II), thus implicating a neutral effect of the cytoplasmic genomes on the amplitude.

Single locus analysis of nuclear variation and the robustness of circadian clock

To further dissect the genomic architecture underlying circadian clock robustness against high temperature in the DH population, a QTL analysis was conducted at three different ways. Initially, we performed a single QTL analysis with the delta between HT and OT for clock FRP and AMP values (dFRP and dAMP, respectively). This also included a di-genic analysis with the possible interaction between nuclear and cytoplasmic loci. In addition, to identify loci associated with trait plasticity, a genetic model containing the QxE component was formulated and probability (P

value) for this interaction of specific loci with the temperature (QxE) was calculated (Sasaki et al., 2015). At last, we hypothesized that the signal to change in the clock rhythm, i.e. one that force the system into conductance of signal to change the clock, may work under a *threshold* model (Falconer, 1965). Under such model an unobservable quantitative variable, termed *liability*, underlying the binary phenotype, with the presence of the abnormality above the threshold and absence below (Falconer 1965). In our case, the significant change in the clock rhythm under heat is the "abnormality". We therefore translated the FRP phenotype of the DH lines into a binary vector (see Methods). This allowed to perform a genome scan for loci that may switch the system from heat compensated [maintaining the same rhythm; (Johnson et al., 2003)] to a responsive one, i.e. one in which the clock rhythm changes up or down.

Single QTL analysis of the delta between HT and OT: For dFRP, setting a manual input of LOD =2.5, which is a relatively permissive threshold for the QTL analysis, led to identifying three QTL (data not shown). However, by increasing the stringency of the genetic analysis using 1000 permutations the threshold LOD became 3.29, leaving a single significant and major QTL on chromosome 2 (*dFRP2.2*, flanked by markers S2H_ 718,338,890 and S2H_722,401,229) that explained 13.4% of variation for the trait, and with additive effect of +1.0 h (the positive value corresponds to allele A vs. B and represent half of the difference between two homozygous genotypes; Fig. 2C; Table S6). The relatively low number of significant QTL underlying the clock plasticity between HT and OT environments was also evident for the dAMP; only a single locus on chromosome 7 (*dAMP7.1*, flanked by markers S7H_498,472,330 and S7H_ 510,903,725) that explained 11.15% of variation for the trait was identified (Fig. 2D; Table S6). We next looked at possible contribution di-genic epistasis interactions to the overall variation of both traits. Performing the di-genic QTL analysis (see Methods) at low stringency (LOD=2.5) identified fifteen pairs of interacting loci, including one in tight vicinity to the single QTL on chromosome 2 (flanked by S2H_706,464,739 and S2H_713,705,096; Table S7). Increasing the stringency to LOD=5 left only two significant di-genic interaction albeit with PVE values below 4% (Table S7). Setting similar stringent threshold of LOD5 for the digenic interactions underlying variation of dAMP concluded with no significant pair of interacting loci, and those found with a LOD2.5 explained each less than 3.5% of the PVE each (Table S7). Notably, this analysis for delta of the clock of both traits did

not identify any significant cytonuclear interaction between the cytoplasm and the nuclear loci.

Markers by environment interaction (QxE) analysis of clock traits: Since the choice of method used for the mapping of trait plasticity has significant consequences on the results (Josephs, 2018) we have used the same dataset of the clock phenotypes of DH population to specifically mapping loci underlying QxE. Indeed, this analysis showed only partial overlap with genome scans of the delta for both traits between environments. For the clock AMP the major QTL on chromosome 7 (*dAMP7.1*) was also identified, at a higher LOD score (5.27) and explaining much more of the variation (PVE=36.43%). This QxE QTL analysis also identified *qeAMP7.3*, an additional QTL on same chromosome between S7H_ 651,765,311 and S7H_656,04,8080 (Fig 2E; Table S6). On the contrary, performing this QxE analysis with the values of the clock FRP did not identify a significant QTL on any chromosome location, nor associated this variation to the cytoplasm.

A threshold-binary model analysis: Our last approach for the QTL analysis stems from the hypothesis of a *threshold* mechanism (see above) and therefore the phenotype of each DH was pre-considered and converted to a categorical binary vector. Per DH line the comparison of FRP means between the two treatments (t Student's test, $p<0.01$) showed that only 12 out of 66 (18.5%) are significantly different for 5009 including negative delta for some lines, while the numbers for 0950 are significantly higher, i.e. 15 out of 34 (44.1%) accelerate their clock under heat (Fig. S4; Fig. 4A). These significant differences (Pearson P>ChiSq=0.004) between two sub-populations are in agreement with the overall robustness of the 5009 vs 0950 DH. This "single locus" analysis for the plasmotype was extended to performing a genome scan of loci affecting the non-random distribution of the binary trait between genotypic groups of each marker (A or B; see Methods). This analysis yielded two QTL on chromosomes 2 and 7 also, but at locations different from loci identified for QxE or the delta of the traits (Fig. 2F; Table S6). The one QTL for environmental response, *erFRP2.1*, on chromosome 2, was flanked between S2H_698,875,542 and S2H_702,308,910 and showed a significant (Pearson P>ChiSq=0.0004) non-random distribution of the binary phenotype, with carriers of the 'A' (B1K-50-09) included 81.6% non-affected, as compared to half of that (40%) among carriers of the 'B' (B1K-09-07) allele (Fig. 4B). Similarly, only 14.8% were affected (changed their FRP under HT compared to OT) among carriers of the 'A' allele at the second QTL

identified using this approach on chromosome 7 QTL, i.e. erFRP7.2 (Fig. 4C). This division between affected and non-affected DH lines was significantly different than the 38.7% affected among B-carriers at this locus (Pearson P>ChiSq=0.014).

Discussion

Automated PAM as a phenomics tool

Given plants' high levels of morphological plasticity, compared to animals, crop phenomics presents distinct challenges (Tardieu et al., 2017). Here, we present a new phenomic tool that allows a non-invasive measurement of the circadian clock rhythm under optimal and high temperature for a large set of genotypes in a relatively short time and with high repetition. This is crucial for QTL mapping or for developing models able to disentangle and simulate plant behavior in a range of habitats. Until very recently, the rhythm of the circadian clock was measured based on expression of genes belonging to the core clock complex, .e.g.CCA and LHY (Gould et al., 2006). This created an obstacle since plants had to be harvested at each time point and therefore either wounded plants were repeatedly sampled (possibly changing the natural condition of the measured plant) or requiring that each genotype be grown in large numbers to allow minimal amount of plants for the statistics. The F method, which requires dark adaptation, possesses some limitations for small labs due to relatively high costs of engineering and manufacturing of the LED panel and CCD camera. Possible alternative for such systems is either to replace or supplement the CCD camera with a thermal one that will capture the leaf temperature. Canopy temperature is known to follow aperture of the stomata, which are also under the control of the circadian clock (Kreps and Kay, 1997). However, one possible caveat of such approach is that recent studies demonstrated differences and possibly independence between the circadian rhythm in stomata cells and the rest of the leaf (Yakir et al., 2011). Further studies are therefore required to make such comparison and combine F and thermal imaging output to provide either a "uniform", organ- or cell-specific rhythms.

Contribution of plasmotype to circadian clock rhythm and its plasticity

In the analysis of the clock characteristics between the two reciprocal sub-populations we found a significant difference in the rhythm and its robustness under changing temperature regimes (Fig. 3). These clear results point to a role of either the chloroplast or mitochondria in regulation of the clock, and indicate the utility of the DH population for dissecting part of the interplay between nuclei and organelles with regard to adjustment of the clock. Most of our knowledge of this interplay underlying circadian clock function though is in the anterograde (nucleus-to-plastid) control of

the organelle, and less on the retrograde (plastid-to-nucleus) signaling. The later is thought to be controlled by the metabolic state of the chloroplast including sugar status (Rolland and Sheen, 2005)(Haydon et al., 2013) and reactive oxygen species. Those are, like sugars, affected in part by photosynthesis in general and under high light in particular (Vandenabeele et al., 2004) or by high temperature. Interestingly, mutation in RNA binding protein destined to the chloroplast resulted with altered circadian rhythms (Hassidim et al., 2007). Nevertheless, the nature of the signal and whether it is circadian-regulated is unknown, but an interesting hypothesis is that circadian regulation of photosynthesis within chloroplasts may cause circadian modulation of a retrograde signal that alters nuclear mRNA (Dodd et al., 2015), including alternative splicing of nuclear-encoded transcripts SR protein (a regulator of RNA splicing) and other splicing factors (Petrillo et al., 2014). However, there are no reports that the sensing and initiation of the signaling for circadian clock plasticity resides within activities in the chloroplast.

The non-synonymous mutations found between the organelle genomes of two donors suggest a relatively low number of candidate genes, if only coding regions are considered as possible causal genes. Our sequencing of the B1K-09-07 and B1K-50-04 plastid genomes identified only 6 non-synonymous mutations, and future studies will have to test if one of these underlies the significant effects of the cytoplasm on circadian clock rhythm. Notably one of the identified non-synonymous reside with the rpoC1 gene, which is part of the PEP protein complex. It is composed of subunits encoded by both plastid (rpoA, rpoB, rpoC1, and rpoC2) and nuclear genes (sig1-6) and coordinated rates of molecular evolution between plastome and nuclear encoded genes were observed, at least in Geraniaceae (Zhang et al., 2015). PEP itself has a wide effect on the plastid transcriptome. PEP controlled genes drive rhythms of transcription from the blue light-responsive promoter of chloroplast-encoded *psbD* (Noordally et al., 2013) and potentially other chloroplast genes. Therefore communicating timing information to the chloroplast genome is proposed to act as a circadian signal (Noordally et al., 2013)(Dodd et al., 2015). Nevertheless, validating such causal variation *in planta* is conditioned on advancing our ability to allow plastid transformation in higher plants, which is timely, yet challenging for monocots (Yu et al., 2017). In addition, despite the relatively low known sequence variation between barley mitochondrial genomes (only 3 SNP, between *H. vulgare* and *H. spontaneum*, including 2 in intergenic regions, out of a genome of 525,599 bp) (Hisano et al.,

2016), we are yet to compare the sequence variation between parental lines to test this variation in this organelle genome as potentially being causal for the differential clock phenotypes among DH sub-populations.

Genetic and biochemical basis for circadian clock plasticity

Flowering time in barley and in other model plants is an example of a research field that gained extensive knowledge from integration of qualitative and quantitative genetics, which assisted to build models to explain the genetics and biochemistry underlying variation between plant populations (see at wikipathways.org/index.php?query=flowering&title=Special%3ASearchPathways&doSearch=1&sa=Search). If QTL approach, rather than forward genetics of mutants, was taken, the trait has been treated a quantitative variable and association was made between allelic and trait variation, which usually was validated by additional mutants in candidate genes(Comadran et al., 2012). Taking the classic QTL approach in our study led to identification of very few QTL that were associated with plasticity or response of the circadian rhythm to high temperature (Fig. 2). This may be the results of having only two possible alleles in our system, as opposed to multiple alleles found in recent multi-parent populations (Maurer et al., 2015)(Merchuk-Ovnat et al., 2018). Nevertheless, the QTL found for FRP and AMP plasticity do not seem to fall on candidate genes in the barley gene pool which were proposed as potential regulators of this trait under domestication (Pankin et al., 2018). Thus, we may have identified, beyond the novel connection to organelle causal variation, some hitherto unknown loci that regulate the clock plasticity under high temperature.

Furthermore, we propose to adopt threshold models, which traditionally were considered for binary disease traits with a polygenic basis (Falconer, 1965)(Xu and Atchley, 1996), to dissect circadian clock plasticity as a binary trait. The main difference from disease phenotypes is the population angle, i.e. in our case the binary score is given based on statistical difference between several individuals of each genotypic group (marker/plasmotype). The biological hypothesis behind this approach is that the signaling to change in the circadian clock as response to elevated temperature work as a semi-conductor, with only a signal above a certain threshold will be amplified and translated to change in the circadian rhythm. From a statistical point of view it adds more confidence since the binary score is based on several individuals. Implying this binary approach has identified different set of loci from the

conventional QTL mapping; in these loci, including the plasmotype, a significant non-random distribution of the affected and non-affected genotypes was found between the two genotypic groups.

CONCLUSIONS

The high-throughput circadian clock analysis of a newly developed reciprocal barley doubled population indicates hitherto unknown relationship between plasmotype variation and thermal phenotypic robustness in a cereal plant model. Additional studies with nearly isogenic lines for the “regular” and “binary” QTL will allow examining the stability of these loci across temperature gradient and with different genetic backgrounds, with the long term goal of identifying the biochemical reasoning underlying allelic differences and their causality. Nevertheless, ongoing work will examine the consequences and relationships between clock phenotypes and whole plant fitness phenotypes under common garden experiment (Hübner et al., 2013). This integrated analysis will question the importance of plasticity vs stability, i.e. canalization (Fridman, 2015), of circadian clock rhythm for plant fitness under fluctuating environment.

Acknowledgements

We wish to thank Royi Levav, Oded Anner and Elad Lifshin (SensyTIV, Israel) for the valuable design, build and implementation of the SensyPAM hardware and software. The technical assistance of Khaled Bishara and Inbar Anner is highly appreciated. The discussions with Prof. Rachel Green and Yuri Dakhiya (The Hebrew University) were instrumental for setting the high-content phenotyping system. The FACCE-ERA-NET (Grant # 406/14) and ISF 1270/17 grants to E.F supported this research. Work of SG is supported by the Max Planck Society.

Conflict of interests

The authors declare that they have no conflict of interest.

Contributions

E.B and E.F. designed the experiments, collected, analyzed and interpreted data, and wrote the manuscript. E.B., A.F. and M.R.P. were involved in the data analysis, its interpretations and assisted in writing the manuscript. T.F. and L.H. generated the doubled haploid population from crosses made by E.F. K.J.S. extracted SNPs from GBS data with assistance of A.F. S.G. sequenced and analyzed the chloroplast genomes.

References

Badr, a, Müller, K., Schäfer-Pregl, R., El Rabey, H., Effgen, S., Ibrahim, H. H., Pozzi, C., Rohde, W. and Salamini, F. (2000). On the origin and domestication history of Barley (Hordeum vulgare). *Mol. Biol. Evol.* **17**, 499–510.

Bedada, G., Westerbergh, A., Müller, T., Galkin, E., Bdolach, E., Moshelion, M., Fridman, E. and Schmid, K. J. (2014). Transcriptome sequencing of two wild barley (*Hordeum spontaneum* L.) ecotypes differentially adapted to drought stress reveals ecotype-specific transcripts. *BMC Genomics* **15**, 995.

Cistué, L., Vallés, M. P., Echávarri, B., Sanz, J. M. and Castillo, A. (2003). Barley anther culture. In *Doubled Haploid Production in Crop Plants: A Manual. eds. Sprin* (ed. Maluszynski, M.), Kasha, K. J.), Forster, P., B.), and Szarejko, I.), pp. 29–34. Amsterdam, the Netherlands: Springer Verlag.

Cloutier, S., Cappadocia, M. and Landry, B. S. (1995). Study of microspore-culture responsiveness in oilseed rape (*Brassica napus* L.) by comparative mapping of a F2 population and two microspore-derived populations. *Theor. Appl. Genet.* **91**, 841–847.

Comadran, J., Kilian, B., Russell, J., Ramsay, L., Stein, N., Ganal, M., Shaw, P., Bayer, M., Thomas, W., Marshall, D., et al. (2012). Natural variation in a homolog of Antirrhinum CENTRORADIALIS contributed to spring growth habit and environmental adaptation in cultivated barley. *Nat. Genet.* **44**, 1388–92.

Dakhiya, Y., Hussien, D., Fridman, E., Kiflawi, M. and Green, R. (2017). Correlations between circadian rhythms and growth in challenging environments. *Plant Physiol.* **173**, 1724–1734.

Dodd, A. N., Salathia, N., Hall, A., Kévei, E., Tóth, R., Nagy, F., Hibberd, J. M., Millar, A. J. and Webb, A. a R. (2005). Plant circadian clocks increase photosynthesis, growth, survival, and competitive advantage. *Science* **309**, 630–633.

Dodd, A. N., Belbin, F. E., Frank, A. and Webb, A. A. R. (2015). Interactions between circadian clocks and photosynthesis for the temporal and spatial coordination of metabolism. *Front. Plant Sci.* **6**, 245.

Edwards, K. D., Lynn, J. R., Gyula, P., Nagy, F. and Millar, A. J. (2005). Natural allelic variation in the temperature-compensation mechanisms of the Arabidopsis thaliana circadian clock. *Genetics* **170**, 387–400.

Ekiz, H., Kiral, A. S., Akçin, A. and Simsek, L. (1998). Cytoplasmic effects on quality traits of bread wheat (*Triticum aestivum* L.). *Euphytica* **100**, 189–196.

Falconer, D. S. (1965). The inheritance of liability to certain diseases, estimated from the incidence among relatives. *Ann. Hum. Genet.* **29**, 51–76.

Frei, U., Peiretti, E. G. and Wenzel, G. (2003). Significance of cytoplasmic DNA in plant breeding. In *Plant Breeding Reviews* (ed. Janick, J.), pp. 175–210. Hoboken: ohn Wiley & Sons, Inc.

Fridman, E. (2015). Consequences of hybridization and heterozygosity on plant vigor and phenotypic stability. *Plant Sci.* **232**, 35–40.

Glaubitz, J. C., Casstevens, T. M., Lu, F., Harriman, J., Elshire, R. J., Sun, Q. and Buckler, E. S. (2014). TASSEL-GBS: A high capacity genotyping by sequencing analysis pipeline. *PLoS One* **9**,.

Gould, P. D., Locke, J. C. W., Larue, C., Southern, M. M., Davis, S. J., Hanano, S., Moyle, R., Milich, R., Putterill, J., Millar, A. J., et al. (2006). The molecular basis of temperature compensation in the Arabidopsis circadian clock.

Plant Cell **18**, 1177–87.

Greenham, K. and McClung, C. R. (2015). Integrating circadian dynamics with physiological processes in plants. *Nat. Rev. Genet.* **16**, 598–610.

Greiner, S. and Bock, R. (2013). Tuning a ménage à trois: Co-evolution and co-adaptation of nuclear and organellar genomes in plants. *BioEssays* **35**, 354–365.

Harlan, J. R. and Zohary, D. (1966). Distribution of wild wheats and barley. *Science* **153**, 1074–80.

Hassidim, M., Yakir, E., Fradkin, D., Hilman, D., Kron, I., Keren, N., Harir, Y., Yerushalmi, S. and Green, R. M. (2007). Mutations in CHLOROPLAST RNA BINDING provide evidence for the involvement of the chloroplast in the regulation of the circadian clock in Arabidopsis. *Plant J.* **51**, 551–562.

Haydon, M. J., Mielczarek, O., Robertson, F. C., Hubbard, K. E. and Webb, A. A. R. (2013). Photosynthetic entrainment of the Arabidopsis thaliana circadian clock. *Nature* **502**, 689–92.

Hisano, H., Tsujimura, M., Yoshida, H., Terachi, T. and Sato, K. (2016). Mitochondrial genome sequences from wild and cultivated barley (Hordeum vulgare). *BMC Genomics* 1–12.

Hubner, S., HÖffken, M., Oren, E., Haseneyer, G., Stein, N., Graner, A., Schmid, K. and Fridman, E. (2009). Strong correlation of wild barley (*Hordeum spontaneum*) population structure with temperature and precipitation variation. *Mol. Ecol.* **18**, 1523–1536.

Hübner, S., Günther, T., Flavell, A., Fridman, E., Graner, A., Korol, A. and Schmid, K. J. (2012). Islands and streams: Clusters and gene flow in wild barley populations from the Levant. *Mol. Ecol.* **21**, 1115–1129.

Hübner, S., Bdolach, E., Ein-Gedy, S., Schmid, K. J., Korol, a. and Fridman, E. (2013). Phenotypic landscapes: Phenological patterns in wild and cultivated barley. *J. Evol. Biol.* **26**, 163–174.

Johnson, C., Elliott, J., Foster, R., Honma, R. and Kronauer, R. (2003). Fundamental properties of circadian rhythms. In *Chronobiology: Biological Timekeeping* (ed. Dunlap, J.), Loros, J. J.), and DeCoursey., P. J.), pp. 67–105. Sinauer Associates, Sunderland, MA.

Joseph, B., Corwin, J. A., Li, B., Atwell, S. and Kliebenstein, D. J. (2013). Cytoplasmic genetic variation and extensive cytonuclear interactions influence natural variation in the metabolome. *Elife* **2013**,.

Josephs, E. B. (2018). Determining the evolutionary forces shaping G × E. *New Phytol.*

Kreps, J. A. and Kay, S. A. (1997). Coordination of plant metabolism and development by the circadian clock. *Plant Cell* **9**, 1235–1244.

Kusakina, J., Gould, P. D. and Hall, A. (2014). A fast circadian clock at high temperatures is a conserved feature across Arabidopsis accessions and likely to be important for vegetative yield. *Plant, Cell Environ.* **37**, 327–340.

Li, H. and Durbin, R. (2009). Fast and accurate short read alignment with Burrows-Wheeler transform. *Bioinformatics* **25**, 1754–1760.

Li, H., Ye, G. and Wang, J. (2007). A modified algorithm for the improvement of composite interval mapping. *Genetics* **175**, 361–374.

Luo, D., Xu, H., Liu, Z., Guo, J., Li, H., Chen, L., Fang, C., Zhang, Q., Bai, M., Yao, N., et al. (2013). A detrimental mitochondrial-nuclear interaction causes cytoplasmic male sterility in rice. *Nat. Genet.* **45**, 573–577.

Mascher, M., Richmond, T. A., Gerhardt, D. J., Himmelbach, A., Clissold, L., Sampath, D., Ayling, S., Steuernagel, B., Pfeifer, M., D'Ascenzo, M., et al.

(2013). Barley whole exome capture: A tool for genomic research in the genus Hordeum and beyond. *Plant J.* **76**, 494–505.

Mascher, M., Gundlach, H., Himmelbach, A., Beier, S., Twardziok, S. O., Wicker, T., Radchuk, V., Dockter, C., Hedley, P. E., Russell, J., et al. (2017). A chromosome conformation capture ordered sequence of the barley genome. 1–43.

Maurer, A., Draba, V., Jiang, Y., Schnaithmann, F., Sharma, R., Schumann, E., Kilian, B., Reif, J. C. and Pillen, K. (2015). Modelling the genetic architecture of flowering time control in barley through nested association mapping. *BMC Genomics* **16**, 1–12.

Meng, L., Li, H., Zhang, L. and Wang, J. (2015). QTL IciMapping: Integrated software for genetic linkage map construction and quantitative trait locus mapping in biparental populations. *Crop J.* **3**, 269–283.

Merchuk-Ovnat, L., Silberman, R., Laiba, E., Maurer, A., Pillen, K., Faigenboim, A. and Fridman, E. (2018). Genome scan identifies flowering-independent effects of barley *HsDry2.2* locus on yield traits under water deficit. *J. Exp. Bot.* **69**,.

Middleton, C. P., Senerchia, N., Stein, N., Akhunov, E. D., Keller, B., Wicker, T. and Kilian, B. (2014). Sequencing of chloroplast genomes from wheat, barley, rye and their relatives provides a detailed insight into the evolution of the triticeae tribe. *PLoS One* **9**,.

Nixon, J. (2006). Testing for segregation distortion in genetic scoring data from backcross or doubled haploid populations. *Heredity (Edinb).* **96**, 290–297.

Noordally, Z. B., Ishii, K., Atkins, K. A., Wetherill, S. J., Kusakina, J., Walton, E. J., Kato, M., Azuma, M., Tanaka, K., Hanaoka, M., et al. (2013). Circadian control of chloroplast transcription by a nuclear-encoded timing signal. *Nature* **339**, 1316–9.

Pankin, A., Altmüller, J., Becker, C. and von Korff, M. (2018). Targeted resequencing reveals genomic signatures of barley domestication. *New Phytol.*

Petrillo, E., Godoy Herz, M. A., Fuchs, A., Reifer, D., Fuller, J., Yanovsky, M. J., Simpson, C., Brown, J. W. S., Barta, A., Kalyna, M., et al. (2014). A chloroplast retrograde signal regulates nuclear alternative splicing. *Science* **344**, 427–30.

Price, T. D., Qvarnstrom, A. and Irwin, D. E. (2003). The role of phenotypic plasticity in driving genetic evolution. *Proc. R. Soc. B Biol. Sci.* **270**, 1433–1440.

Rolland, F. and Sheen, J. (2005). Sugar sensing and signalling networks in plants. *Biochem. Soc. Trans.* **33**, 269–271.

Roux, F., Mary-Huard, T., Barillot, E., Wenes, E., Botran, L., Durand, S., Villoutreix, R., Martin-Magniette, M.-L., Camilleri, C. and Budar, F. (2016). Cytonuclear interactions affect adaptive traits of the annual plant Arabidopsis thaliana in the field. *Proc. Natl. Acad. Sci. U. S. A.* **113**, 3687–92.

Russell, J., Mascher, M., Dawson, I. K., Kyriakidis, S., Calixto, C., Freund, F., Bayer, M., Milne, I., Marshall-Griffiths, T., Heinen, S., et al. (2016). Exome sequencing of geographically diverse barley landraces and wild relatives gives insights into environmental adaptation. *Nat. Genet.* 1–10.

Sanetomo, R. and Gebhardt, C. (2015). Cytoplasmic genome types of European potatoes and their effects on complex agronomic traits. *BMC Plant Biol.* **15**, 162.

Sasaki, E., Zhang, P., Atwell, S., Meng, D. and Nordborg, M. (2015). "Missing" G x E variation controls flowering time in Arabidopsis thaliana. *PLoS Genet.* **11**,.

Schreiber U (2004). Pulse-amplitude-modulation (PAM) fluorometry and saturation

pulse method: an overview. In *Chlorophyll a fluorescence. A signature of photosynthesis* (ed. Papageorgiou, G.), pp. 279–319. Dordrecht: Springer Verlag.

Tardieu, F., Cabrera-Bosquet, L., Pridmore, T. and Bennett, M. (2017). Plant phenomics, from sensors to knowledge. *Curr. Biol.* **27**, R770–R783.

Tillich, M., Lehwark, P., Pellizzer, T., Ulbricht-jones, E. S., Fischer, A., Bock, R. and Greiner, S. (2017). GeSeq – versatile and accurate annotation of organelle genomes. 1–6.

Touraev, A., Forster, B. P., Jain, S. M. and Weyen, J. (2009). Barley and Wheat Doubled haploids in breeding in advances in haploid production in higher plants. 179-187–187.

Vandenabeele, S., Vanderauwera, S., Vuylsteke, M., Rombauts, S., Langebartels, C., Seidlitz, H. K., Zabeau, M., Van Montagu, M., Inzé, D. and Van Breusegem, F. (2004). Catalase deficiency drastically affects gene expression induced by high light in Arabidopsis thaliana. *Plant J.* **39**, 45–58.

Wendler, N., Mascher, M., Nöh, C., Himmelbach, A., Scholz, U., Ruge-Wehling, B. and Stein, N. (2014). Unlocking the secondary gene-pool of barley with next-generation sequencing. *Plant Biotechnol. J.* **12**, 1122–1131.

Xu, S. and Atchley, W. R. (1996). Mapping quantitative trait loci for complex binary diseases using line crosses. *Genetics* **143**, 1417–1424.

Yakir, E., Hassidim, M., Melamed-Book, N., Hilman, D., Kron, I. and Green, R. M. (2011). Cell autonomous and cell-type specific circadian rhythms in Arabidopsis. *Plant J.* **68**, 520–531.

Yu, Q., Lutz, K. A. and Maliga, P. (2017). Efficient plastid transformation in Arabidopsis. *Plant Physiol.* **29**, pp.00857.2017.

Zhang, J., Ruhlman, T. A., Sabir, J., Blazier, J. C. and Jansen, R. K. (2015). Coordinated rates of evolution between interacting plastid and nuclear genes in Geraniaceae. *Plant Cell* **27**, 563–573.

Zielinski, T., Moore, A. M., Troup, E., Halliday, K. J. and Millar, A. J. (2014). Strengths and limitations of period estimation methods for circadian data. *PLoS One* **9**,.

Figures

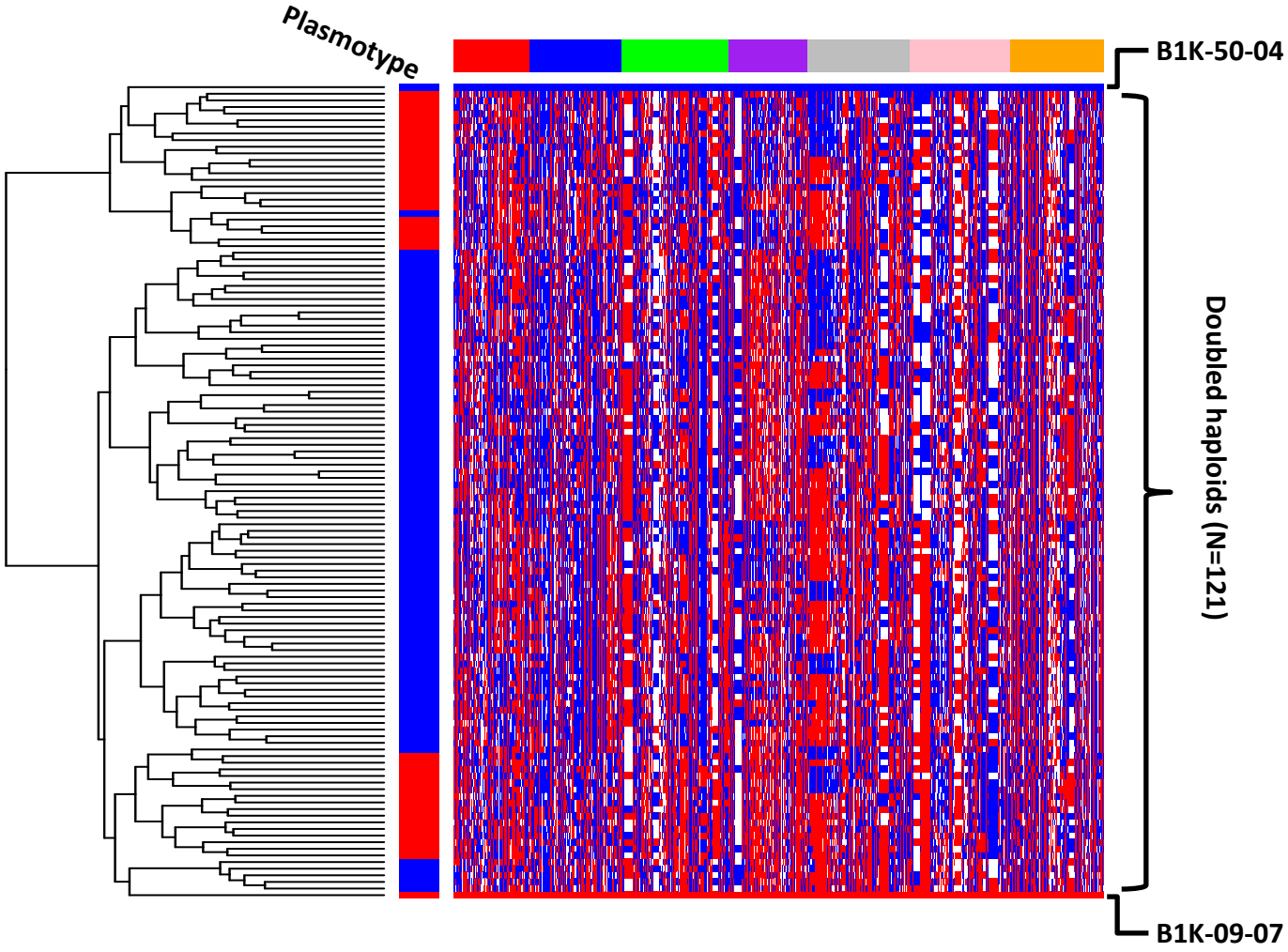

Fig. **1** Graphical representation of allelic distribution of 2237 markers (columns) and 121 doubled haploids (DH) lines (rows). The DH are descended from two single reciprocal F_2 genotypes derived from a cross between B1K-50-04 (blue) and B1K-09-07 (red) and the plasmotype identity of each DH is marked with same color coding.

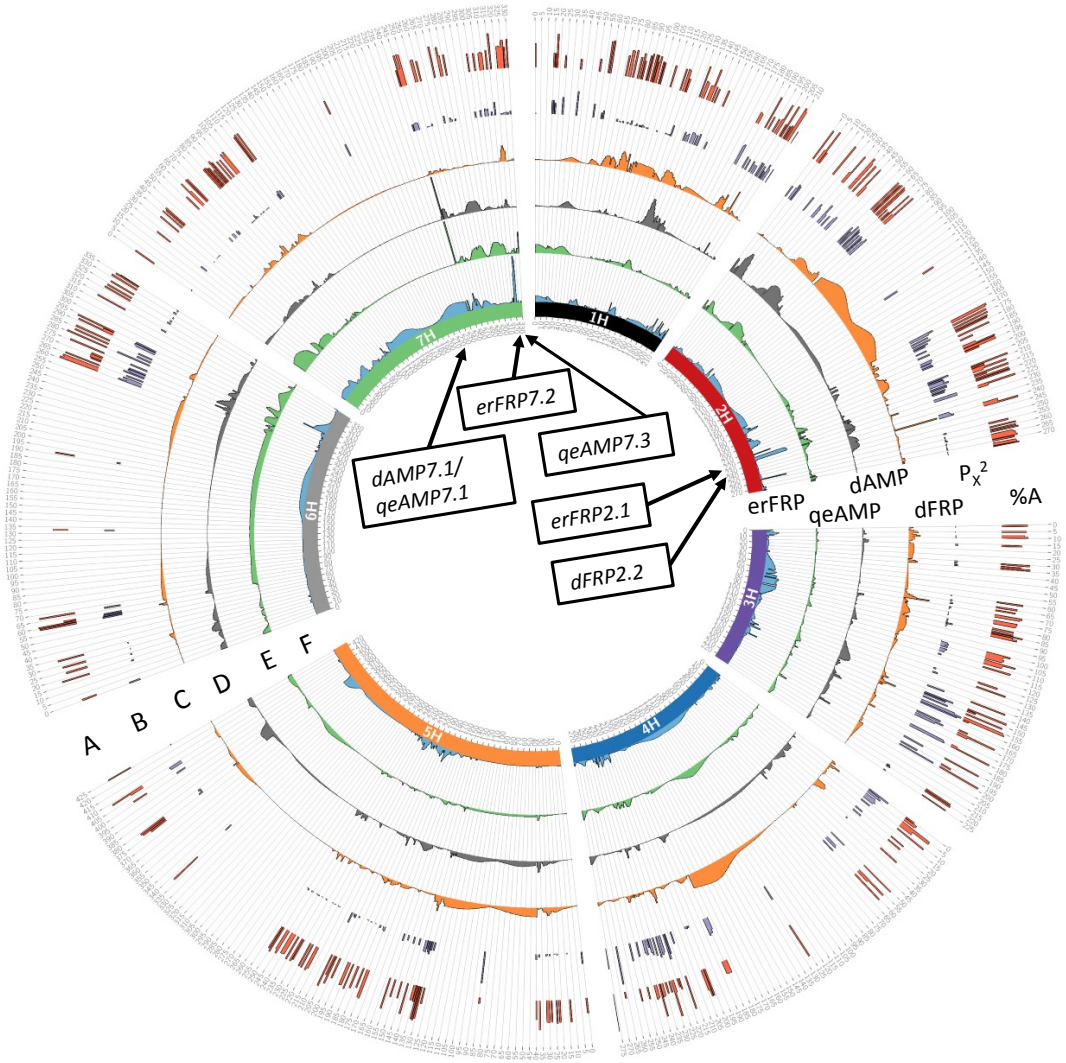

Fig. 2 Circos plot for the allele frequency and QTL analysis results for DH population. (A) Alleles segregation ratios depicted with percentage of the A allele (%A), and (B) statistically tested with a chi-square tests ($-\log_{10}P$) for distortion from expected 1:1 ratio for 760 loci. The QTL results for (C) dFRP, delta free-running period (D) dAMP, delta amplitude (E) qeFRP, QTL by environment interaction, and (F) erFRP, environmental response of FRP, binary-threshold model (see Methods). Barley chromosomes in the Circos plot are depicted in different colors the inner circle. For each trait, the track represents the QTL LOD score in a 1-cM window. Window positions (in cM) are ordered clockwise, per chromosome. The maximum heights of the Y-axis are 89.6 [%], 17.0 [-LogP], 3.13 [LOD], 3.1 [LOD], 5.27[LOD], and 3.86[LOD] for graphs A to F, respectively. Positions and naming of the different QTL are marked with arrow and depicted in the inner circle (see Table S6 for details).

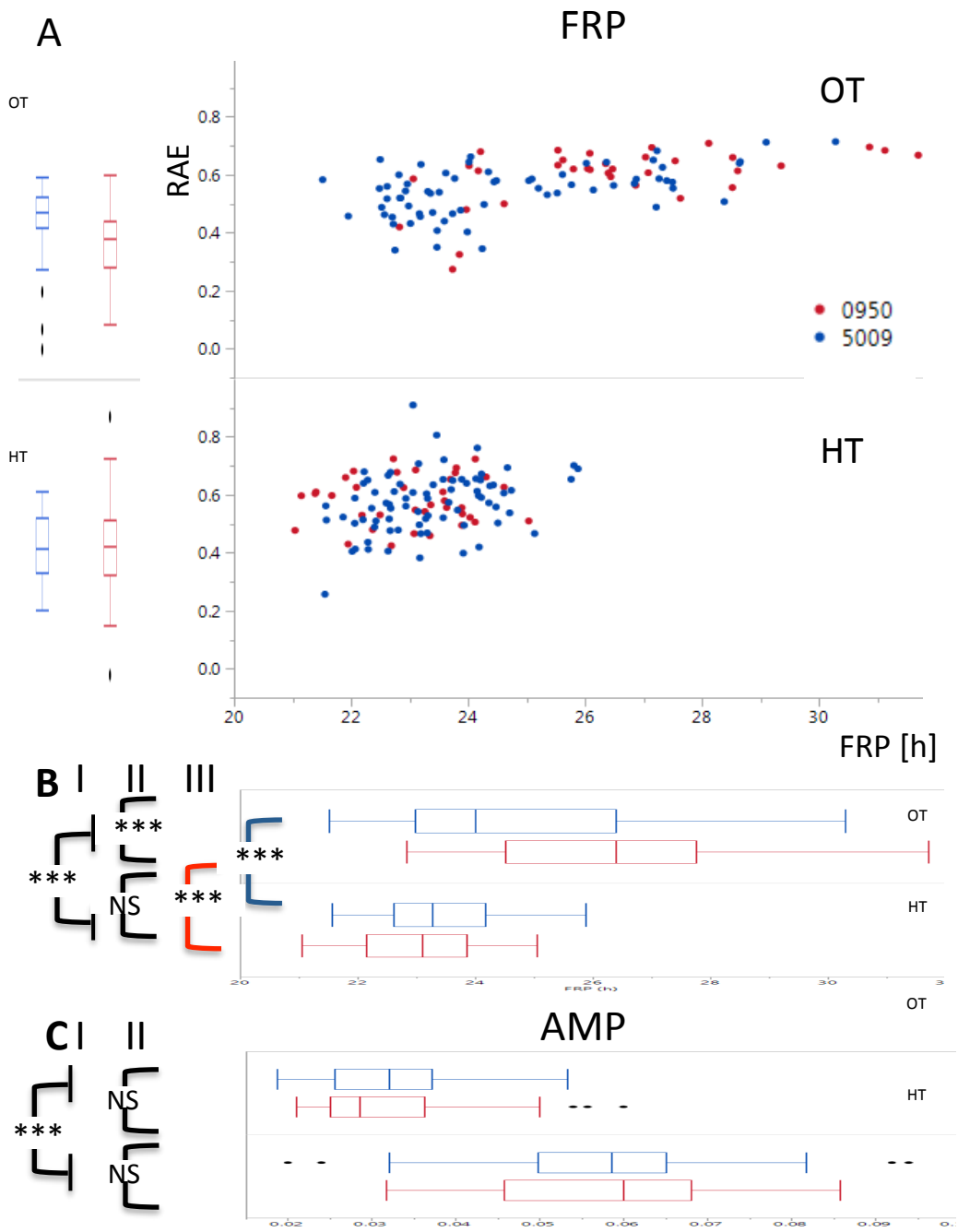

Fig. 3 Circadian clock rhythm in DH plants is differentially shortened under high temperature between carriers of the B1K-09-08 compared to B1K-50-04 plasmotype. (A) Free running period (FRP) vs. relative amplitude error (RAE) of 114 DH lines originated from 2 F_2 reciprocal wild barley, Hybrid_0950 (red) and Hybrid_5009 (blue) under two treatments; optimal temperature (OT) at 22 ^{o}C and high temperature (HT) at 32^{o}C. Mean comparison for (B) FRP and (C) amplitude (AMP) between treatments and between sub-populations. For each t-Test the P value is depicted as ***: P<0.001 or NS: not significant. Test I, Difference between treatments for all population, Test II, Difference between plasmotypes 0950 and 5009 under OT and

HT and Test III, between OT and HT in each subpopulation (0950 and 5009).

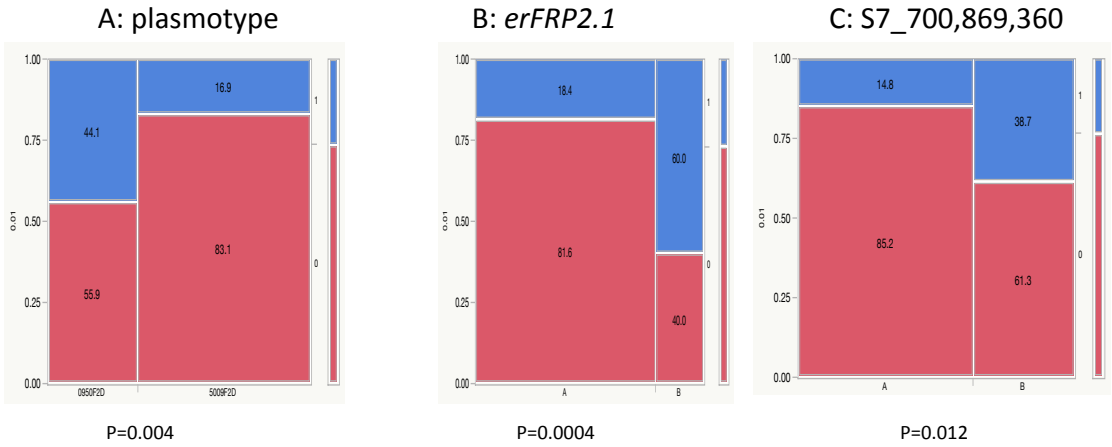

Fig. 4 Distribution of the binary environment-responsive FRP trait (erFRP) between plasmotype and QTL genotypes. (A) Proportion of the affected DH (scored as '1'), i.e. those that show a significant difference (student's t-test; P<0.01) in FRP under HT vs OT, is significantly higher (**χ2** test)in carriers of the B1K-09-07 compared to B1K-50-04 cytoplasm. Similarly, clock rhythm of DH carrying the B1K-50-04 allele in (B) *erFRP2.1* or (C) *erFRP7.2* loci is significantly less affected (scored as '0') compared to those with the B1K-09-07 cytoplasm. Pearson P value of **χ2** test for each locus is indicated below.